Co-doped V_2O_5 nanozyme with excellent peroxidase- and oxidase-like activities for efficient degradation of oxytetracycline without activator

Li Ruiyi, Yang Chen and Li Zaijun*

Key Laboratory of Synthetic and Biological Colloids, Ministry of Education, School of Chemical and Material Engineering, and School of Life Science and Health Engineering, Jiangnan University, Wuxi 214122, China

1 Apparatus

Transmission electron microscope (TEM) images were conducted on JEOL 2010 FEG microscope at 200 keV. Fluorescence spectrum and intensity were measured on a Cary Esclipse fluorescence spectrophotometer (Agilent, Japan). Atomic force microscopic (AFM) images were taken by Multimode 8 Force Microscope (Bruker, Germany). Infrared spectra (IR) were recorded by Nicolet FT-IR 6700 spectrometer (Thermo Fisher Scientific Co., Ltd., America). UV-visible spectra were recorded on a TU-1901 spectrometer with DH-2000 deuterium and tungsten halogen light source in the absorbance mode (Beijing Purkinje General Instrument Co., Ltd., China). X-ray photoelectron spectroscopic (XPS) measurements were performed on the ESCALAB 250Xi photoemission spectrometer having Al K_α (1486.6 eV) dual anode as the source operating at 14.6 kV of anode voltage and 13.5 mA filament current. The XPS data was collected with pass energy of 20 eV at $4xl0^{-9}$ m bar vacuum. Initially the XPS unit was calibrated using Fermi edge of Ag (KE 1482.544). The C 1s line of adventitious carbon with BE = 284.8 eV was taken as a reference for surface-charging corrections. The core-level spectra were decomposed into their components with mixed Gaussian-Lorentzian lines by a non-linear least squares curve-fitting procedure, using the CasaXPS software. The binding energies and FWHM of the peaks were determined from the fitting results. The polyacrylamide gel electrophoresis (PAGE) was imaged with BIO-RAD ChemiDoc XRs

2 Steady-state dynamic parameter measurement

Steady-state dynamic parameters for oxidation of 3,3′,5,5′-tetramethylbenzidine (TMB) in the presence of H_2O_2 under the catalysis of RSB-GQD@V_2O_5-Co were measured by varying the concentrations of H_2O_2 and TMB. When H_2O_2 was used as the substrate, the reaction system containing 0.1 mL of 10 mM TMB, 0.775 mL of acetate buffer solution of pH 4 and 0.1 mL of the H_2O_2 solution with different concentration was mixed with 25 μL of 1 mg mL^{-1} RSB-GQD@V_2O_5-Co dispersion. Subsequently, its change in the absorbance at 642 nm was monitored by spectrophotometer. When TMB was used as the substrate, the reaction system containing 0.1 mL of 10 mM H_2O_2, 0.775 mL of acetate buffer solution of

pH and 0.1 mL of the TMB solution with different concentration was mixed with 25 μL of 1 mg mL^{-1} RSB-GQD@V_2O_5-Co. Subsequently, its absorbance at 642 nm was monitored by spectrophotometer. The absorbance at 642 nm was used for calculating steady-state dynamic parameters by Lineweaver-Burk equation (1). In the equation, V, V_{max}, [S] and K_M present initial reaction rate, maximum reaction rate, substrate concentration and Michaelis-Menten constant, respectively. The above procedure was also used for calculating steady-state dynamic parameters for oxidation of TMB in the absence of H_2O_2 under catalysis of RSB-GQD@V_2O_5-Co unless the replacement of H_2O_2 solution with an equal volume of the acetate buffer solution of pH 4.0.

$$\frac{1}{V} = \frac{K_M}{V_{max}} \times \frac{1}{[S]} + \frac{1}{V_{max}} \quad (1)$$

3 Specific catalytic activity evaluation

To evaluate the peroxidase-like activity of RSB-GQD@V_2O_5-Co, the mixed solution containing 0.1 mL of 10 mM TMB, 0.1 mL of 10 mM H_2O_2 and 0.775 mL of the acetate buffer solution (pH 4) was prepared. After 0.1 mL of 25 μL of the RSB-GQD@V_2O_5-Co dispersion with different concentration, its absorbance at 652 nm and visible absorption spectrum were monitored by spectrophotometer. Further, the activity of RSB-GQD@V_2O_5-Co as the peroxidase-like nanozyme (b, U) was calculated by the equation (2).

$$b = \frac{V}{\varepsilon \times L} \times \frac{\Delta A}{\Delta t} \quad (2)$$

In the equation, V, ε, L and ΔA/Δt presents the volume of reaction system, molar absorption coefficient of TMB (39000 M^{-1} cm^{-1}), optical length of cell and change rate of the absorbance at 642 nm with the reaction time, respectively. The specific activity of RSB-GQD@V_2O_5-Co (a, U mg^{-1}) was calculated by the equation (3).

$$a = \frac{b}{m} \quad (3)$$

In the equation, m presents the mass (mg) of RSB-GQD@V_2O_5-Co in the reaction system. The above procedure was also used for evaluating the oxidase-like activity of RSB-GQD@V_2O_5-Co unless the replacement of H_2O_2 solution in the model reaction system by an equal volume of the acetate buffer solution.

4. Figures and Tables

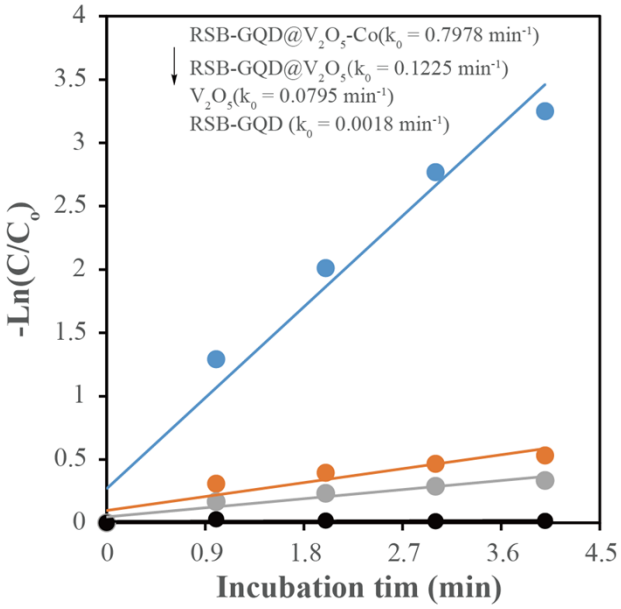

Fig. s1 Plots of -Ln(C/C_0) *vs*. the incubation time under the catalysis of RSB-GQD, V_2O_5, RSB-GQD@V_2O_5, and RSB-GQD@V_2O_5-Co

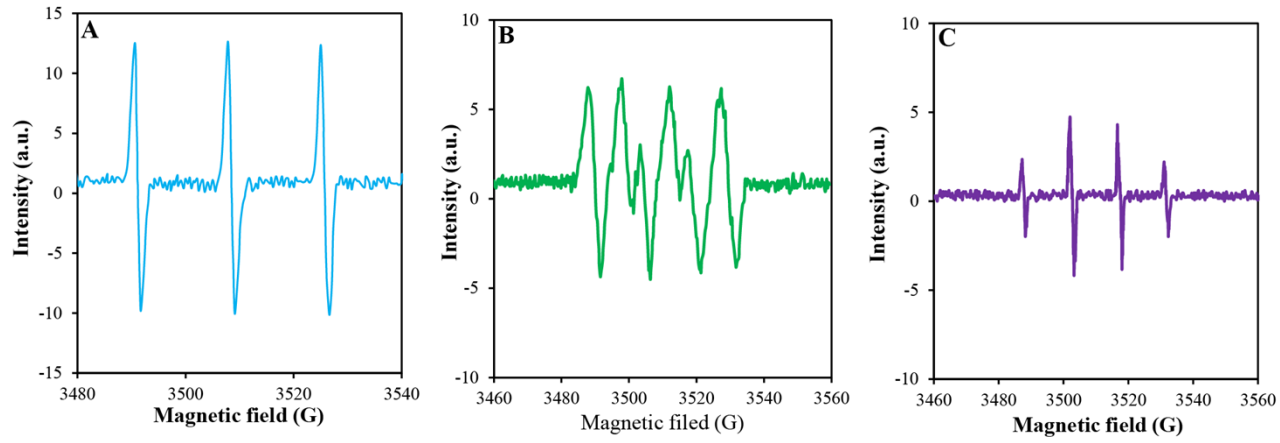

Fig. s2 ESR spectra of radical adducts of DMPO-•OH (A), DMPO-$^{\bullet}O_2^-$ (B) and TEMP-$^1O_2$ (C)

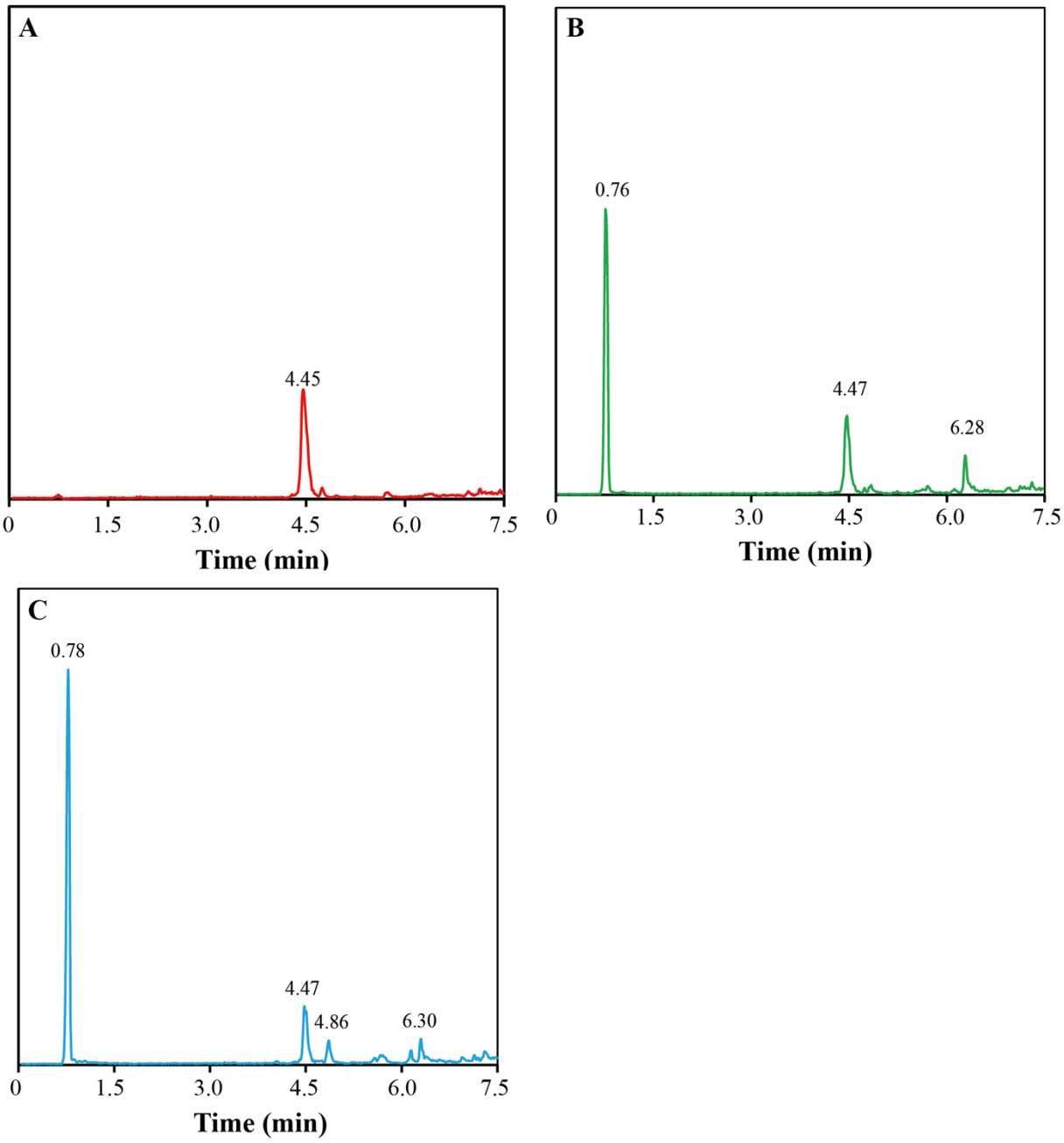

Fig. s3 HPLC chromatograms of the oxytetracycline solution before (A) and after degraded 1 min (B) and 10 min (C) under catalysis of RSB-GQD@V_2O_5-Co

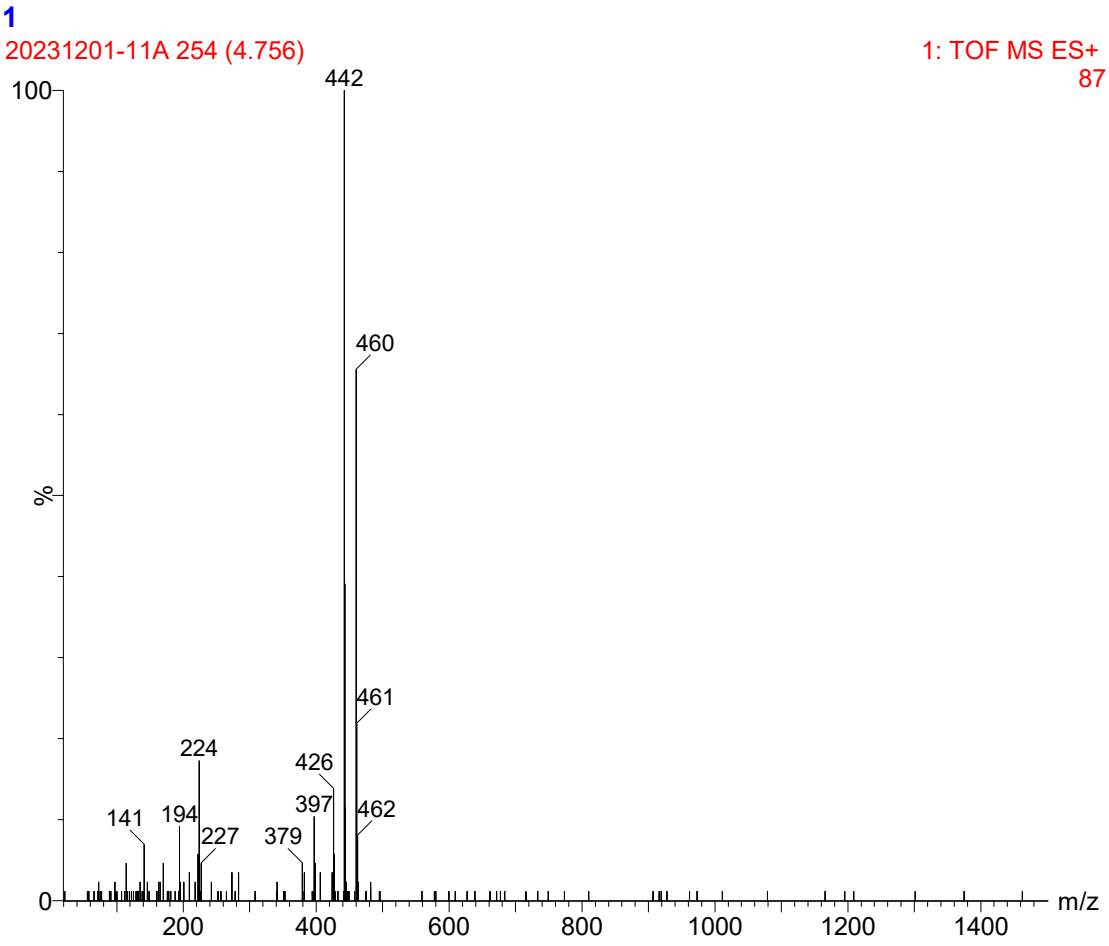

Fig. s4 Mass spectrum of the oxytetracycline solution before degraded under catalysis of RSB-GQD@V_2O_5-Co

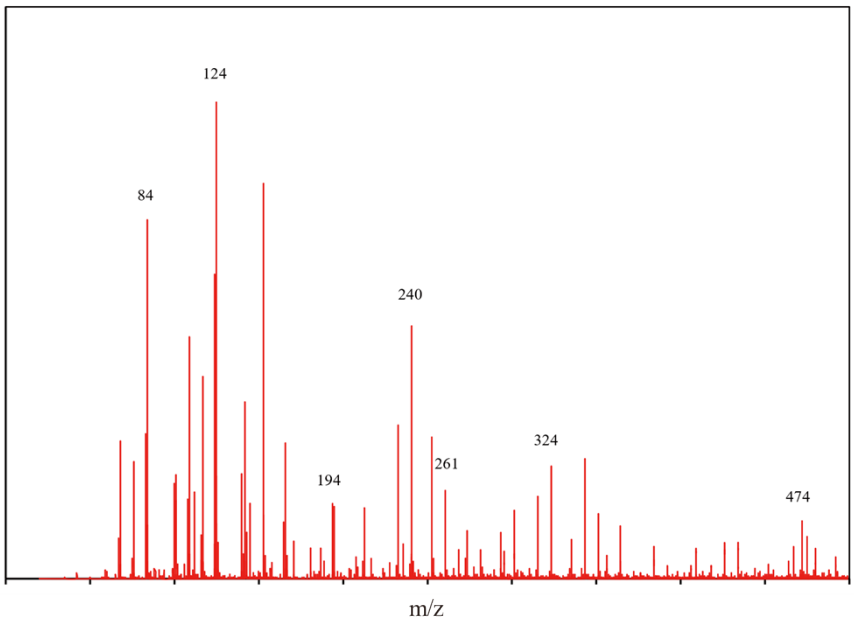

Fig. s5 Mass spectrum of HPLC peak at 0.76 min of retention time

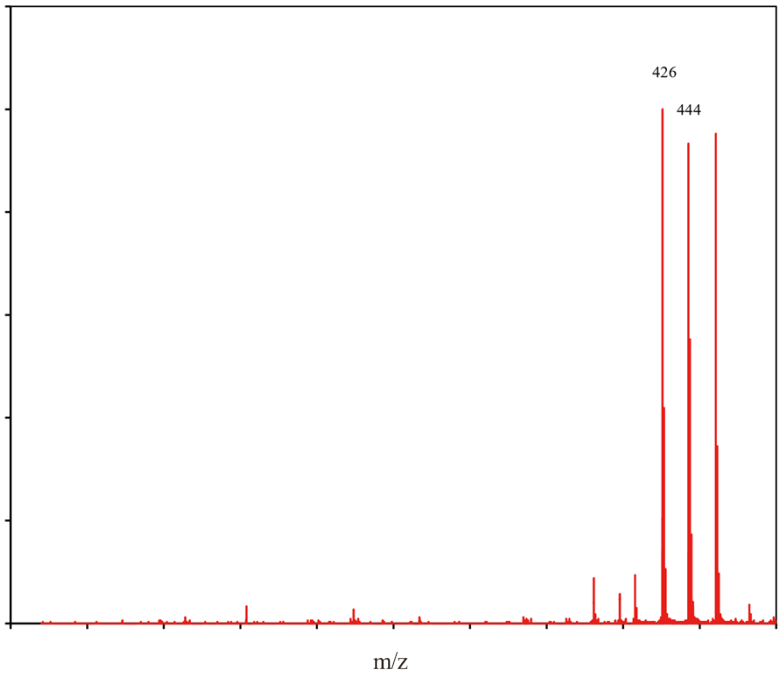

Fig. s6 Mass spectrum of HPLC peak at 4.47 min of retention time

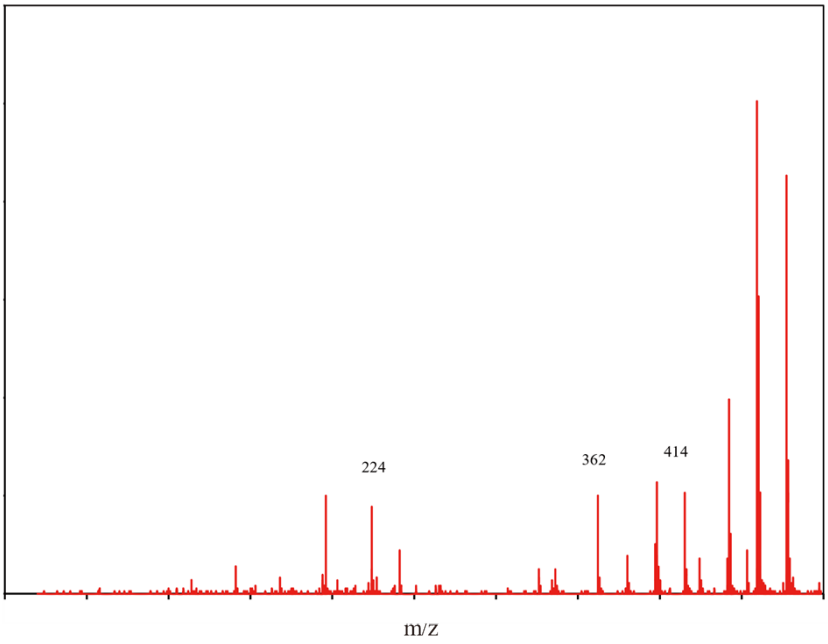

Fig. s7 Mass spectrum of HPLC peak at 6.28 min of retention time

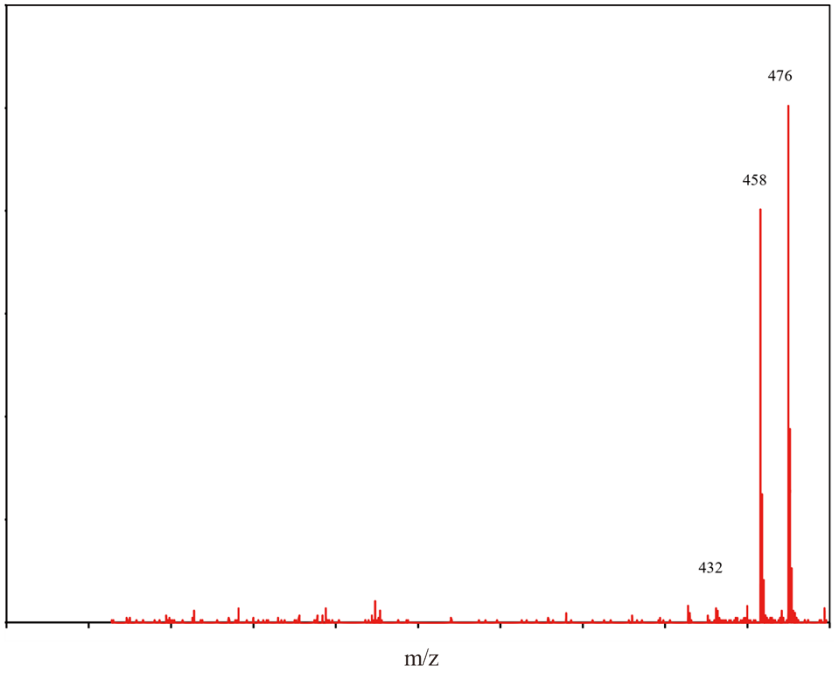

Fig. s8 Mass spectrum of HPLC peak at 0.78 min of retention time

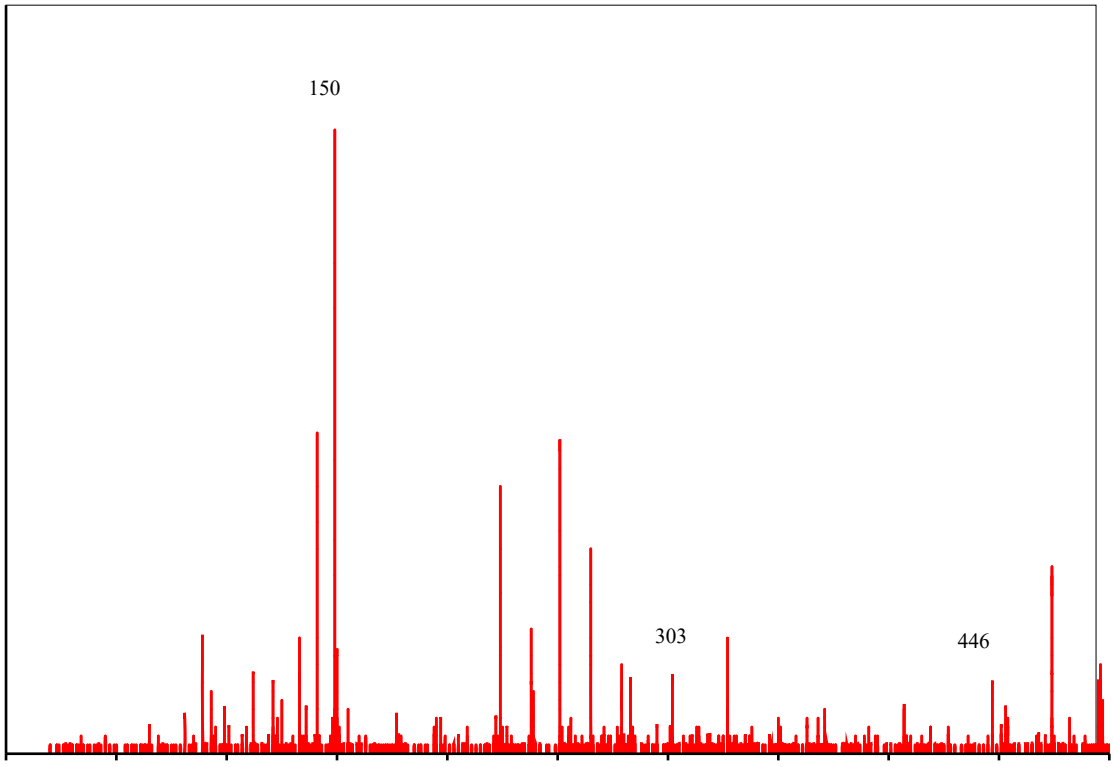

Fig. s9 Mass spectrum of HPLC peak at 6.30 min of retention time

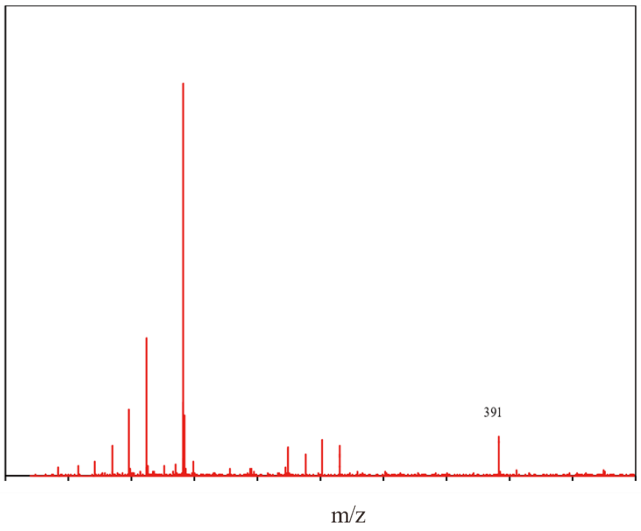

Fig. s10 Mass spectrum of HPLC peak at 4.86 min of retention time

Table s1 EIS of the electrode modification process

Electrode modification process	R_S（Ω）	R_{ct}（Ω）	Capcitance(F)	Warburg,Yo
V_2O_5	6.084	133.9	1.04E-4	0.002994
GQD-V_2O_5	5.619	14.1	9.388E-5	0.04668
GQD-V_2O_5-Co	7.477	1.231	2.677E-4	0.06722

Table s2 Comparison of catalytic activity of different nanozymes

Nanozyme	Enzyme-like activity	Specific activity (U mg^{-1})	Temperature (°C)	Ref.
Fe_2O_3/carbon nanotubes	Peroxidase-like	25.4	37	[1]
Cellulose nanofibrils-supported PdNPs	Peroxidase-like	0.415	30	[2]
	Oxidase-like	0.277	30	
Fe,N co-doped ultrathin hollow carbon framework	Peroxidase-like	36.6	40	[3]
N doped carbon	Peroxidase-like	6.3	40	[4]
Fe,N co-doped carbon	Peroxidase-like	15.2	40	[4]
PdNPs/ TEMPO-oxidized cellulose nanofibril	Peroxidase-like	0.215	30	[4]
	Oxidase-like	0.107	30	

Prussian blue nanoparticles	Peroxidase-like	465.8	37	[5]
Fe single-atom/Pt clusters	Peroxidase-like	87.7	37	[6]
AuPtCo	Peroxidase-like	27.1	Room temperature	[7]
RSB-GQD@V_2O_5-Co	Peroxidase-like	893.35	25	This work
	Oxidase-like	125.95	25	

5 References

[1]. Y. C. Yang, T. Li, Y. Qin, L. B. Zhang and Y. Chen, Construct of Carbon Nanotube-Supported Fe_2O_3 Hybrid Nanozyme by Atomic Layer Deposition for Highly Efficient Dopamine Sensing, Front. Chem., 2020, 8, 564968. https://doi.org/10.3389/fchem.2020.564968

[2]. R. Dadigala, R. Bandi, M. Alle, C. W. Park, S. Y. Han, G. J. Kwon and S. H. Lee, Effective fabrication of cellulose nanofibrils supported Pd nanoparticles as a novel nanozyme with peroxidase and oxidase-like activities for efficient dye degradation, J. Hazard. Mater., 2022, **436**, 129165. https://doi.org/10.1016/j.jhazmat.2022.129165.

[3]. J. Y. Hao, C. Zhang, C. X. Feng, Q. Wang, Z. Y. Liu, Y. Li, J. S. Mu, E. C. Yang and Y. Wang, An ultra-highly active nanozyme of Fe,N co-doped ultrathin hollow carbon framework for antibacterial application, Chinese Chem. Lett., 2023, 34, 107650. https://doi.org/10.1016/j.cclet.2022.06.073.

[4]. R. Dadigala, R. Bandi, S. Y. Han, G. J. Kwon and S. H. Lee, Rapid in-situ growth of enzyme-mimicking Pd nanoparticles on TEMPO-oxidized nanocellulose for the efficient detection of ascorbic acid, Int. J. Biol. Macromol., 2023, 234, 123657. https://doi.org/10.1016/j.ijbiomac.2023.123657.

[5]. Z. G. Qin, B. Chen, Y. Mao, C. Shi, Y. Li, X. Huang, F. Yang and N. Gu, Achieving Ultrasmall Prussian Blue Nanoparticles as HighPerformance Biomedical Agents with Multifunctions, ACS Appl. Mater. Interfaces, 2020, 12, 57382-57390. https://dx.doi.org/10.1021/acsami.0c18357.

[6]. Y. F. Chen, L. Jiao, H. Y. Yan, W. Q. Xu, Y. Wu, L. R. Zheng, W. L. Gu and C. Z. Zhu, Fe−N−C Single-Atom Catalyst Coupling with Pt Clusters Boosts Peroxidase-like Activity for Cascade-Amplified Colorimetric Immunoassay, Anal. Chem., 2021, 93, 12353-12359. https://doi.org/10.1021/acs.analchem.1c02115.

[7]. X. Y. Zhou, C. Fan, Q. W. Tian, C. H. Han, Z. Q. Yin, Z. Y. Dong and S. Bi, Trimetallic AuPtCo Nanopolyhedrons with Peroxidase- and Catalase-Like Catalytic Activity for Glow-Type Chemiluminescence Bioanalysis, Anal. Chem., 2022, 94, 847-855. https://doi.org/10.1021/acs.analchem.1c03572.